Investigation of Rosemary Active Ingredients as COVID-19 Inhibitors: Molecular Docking and DFT

Talaat H. Habeeb

Biology Department, Faculty of Science at Yanbu, Taibah University
King Khalid Rd., Al Amoedi, 46423 (Yanbu El-Bahr, Saudi Arabia)
Email: Thabeeb [AT] taibahu.edu.sa

ABSTRACT— ***Rosemary is an important type of the natural Lamiaceae plant family with several medicinal properties, rendering it as a prospective inhibitor for the new SARS-CoV-2 virus. Its SARS-CoV-2 inhibition properties has not yet been reported. In this study the inhibition efficacy of rosemary against SARS-CoV-2 has been demonstrated using molecular docking along with systematic density-functional-theory (DFT) calculations. The estimated DFT data have shown that the dipole moment of rosemary active ingredient was in the range of 4.29-1.68 with the highest value attained by the carnosic acid. The high dipole moment for the carnosic acid may indicate its appropriate binding affinity pose within a specific virus target receptor. Moreover, the structural complexity for the carnosic acid gave rise to its highest calculated polarizability of 225.5 Bohr^3 compared to the rest of the rosemary ingredients. Remarkably, the carnosic acid active ingredient has the least energy gap between the frontier orbitals (highest occupied molecular orbital (HOMO) and lowest unoccupied molecular orbital (LUMO)) of ~ 5.43 eV, with several hydrophilic sites for interactions, further enabling its binding with the virus receptors. Interestingly, and as anticipated from DFT results, molecular docking calculations showed that carnosic acid had the least binding energy (−6.9 kcal/mol) and, hence, can be regarded as a prospective inhibitor to SARS-CoV-2 main protease (M^{pro}). It binds to both M^{pro} catalytic dyads (Cys-145 and His-41) with hydrogen bond and π-interaction. This carnosic acid ligand binding quality was comparable to renowned SARS-CoV-2 drugs, hydroxychloroquine and favipiravir, having binding affinities of −6.1 and −5.1 kcal/mol, respectively.***

Keywords— COVID-19, rosemary, molecular docking, DFT calculations

1. INTRODUCTION

Currently the world is facing the worst global health crisis by the newly discovered Coronavirus disease 2019 (COVID-19), an infectious disease caused by severe acute respiratory syndrome (SARS-CoV-2). Local hospitals in Wuhan reporting severe pneumonia of unknown cause in December 2019. In February 2019 researchers found that 96% of COVID-19 is shared with a bats genetic material. This disease is mainly transmitted from person to person by contact with discharge from the nose projected to air when infected people sneeze, talk or cough, or by contact with droplets of saliva. This condition is also spread by infected hands. The most popular symptoms are sore throat, fever, cough, fatigue and breathlessness. The incubation period for this virus varies from 2 to 14 days. In addition, the characteristics of this virus make prevention really complicated.

Until 3rd of November 2020, based on information from the world health organization (WHO), more than 46 million cases of SARS-CoV-2 disease with 1,196362 deaths have been reported. At the same time the Saudi Arabi has reported to WHO, 348.037 confirmed cases of COVID-19 and 5437 deaths. In the mid-1960s, first discovery of human coronaviruses was observed (Nishiura, Linton, and Akhmetzhanov 2020; Zhou, Zhang, et al. 2020). It belongs to the Coronaviridae family, which is enveloped positive strand RNA virus. This virus family is classified into 4 genera (α, β, γ, and δ). Types α and β commonly affect humans and mammals whereas the other genera mainly infect birds (Zhu et al. 2020). COVID-19 has crown-shape spikes; it is a novel virus of the β genus; it is spherical with a radius of ≈ 30 -70 nm (Zhu et al. 2020). Because of fast spreading epidemic and the current health and economic concerns, several scientific organizations have been motivated to dig for efficient and safe vaccination or medication for it. An ongoing pandemic with COVID-19 has posed substantial challenge for scientific research in all over the World after the World Health Organization could not rule out airborne transmission of corona virus (Zhou et al. 2020). So far, there are no globally accepted vaccine or non-toxic specific antiviral treatments for this disease. Therefore, all countries must rely on the introduction of serious prevention and control procedures to reduce the hazard of infection transmission (Liu et al. 2020). In the absence of cure for this virus, the door became widely open for urgent alternative approaches to control the spread of the infection. Especially after it was confirmed that COVID-19 is a single-stranded RNA genome and covered through

folded structure (Yao et al. 2020). Backbone approaches is useful and possible for many researchers. To better face this global challenge, the investigation of the computational methods and fascinating pharmacophore is a promising path (Shetty et al. 2020). In general, the core principles for the infectionprevention and management are the avoidance of the cause of infection and the protection of the most susceptible population (Yang and Wang 2020). The hydroxychloroquine, an approved medication for malaria disease by Food and Drug Administration (FDA), was explored as a medication for COVID-19 (Yao et al. 2020; Liu, Cao, et al. 2020). Previous study disclosed that, hydroxychloroquine and chloroquine hinder the COVID-19 by modifying the pH level at the cell membrane surface. This modification hinders the binding of the coronavirus to the cell membrane. Moreover, it hinders glycosylation of viral proteins, nucleic acid replication, virus release, virus particle delivery, and other mechanisms (Grimstein et al. 2019). Ebola's drug Remdesivir (Devaux et al. 2020), has demonstrated activity against the coronavirus family (Warren et al. 2016; Wang et al. 2020).

Several domestic and international academic agencies and corporations have used a variety of approaches, including recombinant or inactivated vaccine technology, mRNA nano-vaccine technology, and DNA vaccine technology, in order to develop COVID-19 vaccine (Yang and Wang 2020). However, hitherto, there are no globally approved COVID-19 vaccines available. In other words, the treatment of coronavirus has not proven availability of an antiviral agent. Therefore, the current work indicates that choice of certain moieties with the necessary viral restraining mechanisms can deliver encouraging outcomes. During the last two decades, there was widespread development in the biomedical research has remained relatively limited of the annual number of novel treatments approved by the FDA (Avorn 2015). In comparison existing clinical protocols, the drug repurposing for virus such as Sars-Cov-19 is signified as an important drug discovery plan from existing medications and reduce the cost and could essentially shorten the time (Cheng 2019; Cheng et al. 2017; Cheng, Murray, and Rubin 2016; Zhou, Hou, et al. 2020; Liu, Zhou, et al. 2020; Shetty et al. 2020). Recently, traditional chinese medicinal plants were identified as Sars-Cov-19 inhibitors (Zhang and Liu 2020; Chan, Wong, and Tang 2020). Rosemary, or rosmarinus officinalis, is a natural plant associated with the Lamiaceae group which is a 1-m height green plant with a specific aroma. Its derivatives (specifically from the leaves) have long been considered a popular medicinal herbal product acting, for instance, as anti-oxidant agent in food conservation and other applications (Cui et al. 2012; Pérez-Fons, GarzÓn, and Micol 2010). Rosemary has been adopted as an effective medicinal plant for treatments of diabetes, hypertension, etc … (Amel 2013; Javanmardi et al. 2003). Recently it has been proved to have pharmaceutical activities such as antibacterial, anticancer (Cheung and Tai 2007; Yesil-Celiktas et al. 2010) antidiabetic (Bakırel et al. 2008) and antidiuretic (Haloui et al. 2000). Chemical content inspection of the rosemary derivatives revealed that the most pharmacologically active composition is the canosic acid amongst the others, including, Borneol, Eucalyptol, Camphor, Carnosol (Elhassan and Osman 2014; Al-Sereiti, Abu-Amer, and Sena 1999; Borrás-Linares et al. 2014; Tu et al. 2013). The first extraction of the carnosic acid from the rosemary was in 1965 (Wenkert, Fuchs, and McChesney 1965). Research have shown that it dominates the composition of the rosemary by about 2-3% of the dried leaves (Wenkert, Fuchs, and McChesney 1965). Therefore, rosemary, through its active carsonic acid ingredient, can be considered as a potential medicinal plant with wide pharmaceutical spectrum against various diseases. To the best of our knowledge, this plant has not been considered for the inhibition of Sars-Cov2.

This paper will, thus, present systematic computational calculation based of DFT and molecular docking to demonstrate the binding efficiency of selected rosemary derivatives (Carnosic acid, Borneol, Eucalyptol, and Camphor) on the Sars-Cov2 main protease (M^{pro}). As anticipated, our calculations showed that the carnosic acid attained the most desirable drug properties (as compared to the rest of the derivatives and the famous hydroxychloroquine and lopinavir), rendering it a potential drug ligand for binding on the Sars-Cov2 M^{pro}.

2. RESULTS AND DISCUSSION

2.1 DFT Theoretical Calculations

The theoretical calculations by the DFT were achieved by B3LYP 6-311G (d,p) basis set. All optimal structures of the active ingredient of rosemary (Figure 1) are proved to be stable, which is confirmed by the lack of the imaginary frequency. The theoretical DFT calculation outcomes for studied compounds presented the non-coplanarity structures. Table 1 summaries the DFT calculated dipole moment, thermal parameters, and the polarizability of the drug's active ingredients.

The estimated DFT data showed that the dipole moment of the active ingredient of rosemary under investigation was in the range of 4.29-1.68 and in the order of carnosic acid > camphor > borneol > eucalyptol. The high dipole moment of carnosic acid and eucalyptol could explain their good binding affinity position within an explicit target receptor. The result of their predicted binding type is further discussed in the molecular docking section. The polarizability of these active ingredients will be determined by how the liability of the electron of these systems is affected by a charge approaching during an electronic process. Moreover, such polarizability is dependent on the complexity and size of the molecular structure of the compounds. Bigger size molecules are more polarizable than the smaller ones. Furthermore,

the compound eucalyptol has the least polarizability (104.5 $Bohr^3$), however, carnosic acid with the most complexity has the highest polarizability, 225.5 $Bohr^3$.

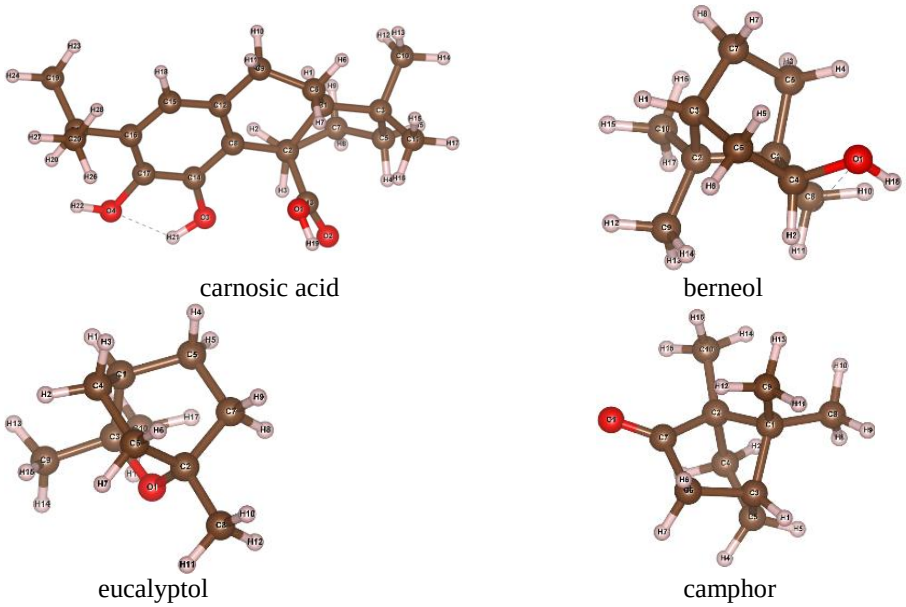

Figure 1: Optimized structures of carnosic acid, berneol, eucalyptol, and camphor with atomic numbering.

Table 1: Thermal parameters (Hartree), dipole moment (Debye), and polarizability α ($Bohr^3$) of carnosic acid, berneol, eucalyptol, and camphor.

Parameter	Carnosic acid	Borneol 64685	Eucalyptol 2758	Camphor 2537
Ecorr	0.47	0.28	0.28	0.25
ZPVE	-1078.75	-466.52	-466.54	-465.35
Etot	-1078.72	-466.51	-466.53	-465.34
H	-1078.72	-466.50	-466.52	-465.34
G	-1078.79	-466.55	-466.57	-465.38
Total Dipole Moment	4.29	1.75	1.68	3.24
Polarizability α	226.52	107.56	108.83	104.48

ZPVE: Sum of electronic and zero-point energies; E_{tot}: Sum of electronic and thermal energies; H: total enthalpies; G: total free energies.

2.2 Frontier Molecular Orbitals (FMOs)

FMOs are the lowest unoccupied molecular orbital (LUMO) and the highest occupied molecular orbital (HOMO). The HOMO is responsible for electron donation, while, LUMO for electron acceptance. The energy levels of these orbitals dominate the interaction mode of the drug like compounds with neighbor receptors, for example the interactions between these compounds and the target proteins. The FMO can provide qualitative information regarding electron sensitivity and transfer from HOMO to LUMO of the other compound. Furthermore, HOMO and LUMO are important chemical reactivity descriptors. The energy levels between the HOMO and LUMO of the investigated active ingredient of rosemary were calculated using DFT method at B3LYP 6-311G (d,p) basis set and are presented in Table 2. The HOMO and LUMO isodensity 2D plots for drugs are shown Figure 2.

Table 2: Calculated HOMO and LUMO energies, electronegativity (χ), global hardness (η), global electrophilicity index (ω), softness (δ), the ionization potential (I) and the electron affinity (A) (in eV) of the compounds investigated: carnosic acid, berneol, eucalyptol, and camphor.

Ingredient	Carnosic acid	Borneol	Eucalyptol	Camphor
EHOMO	-5.68	-7.00	-6.39	-6.43
ELUMO	-0.25	-0.67	-0.76	-0.55
ΔE	5.43	7.67	7.15	5.88
χ	2.96	3.17	2.82	3.49
η	2.72	3.83	3.57	2.94
δ	0.37	0.26	0.28	0.34
ω	1.62	1.31	1.11	2.08
I	5.68	7.00	6.39	6.43
A	0.25	0.67	0.76	0.55

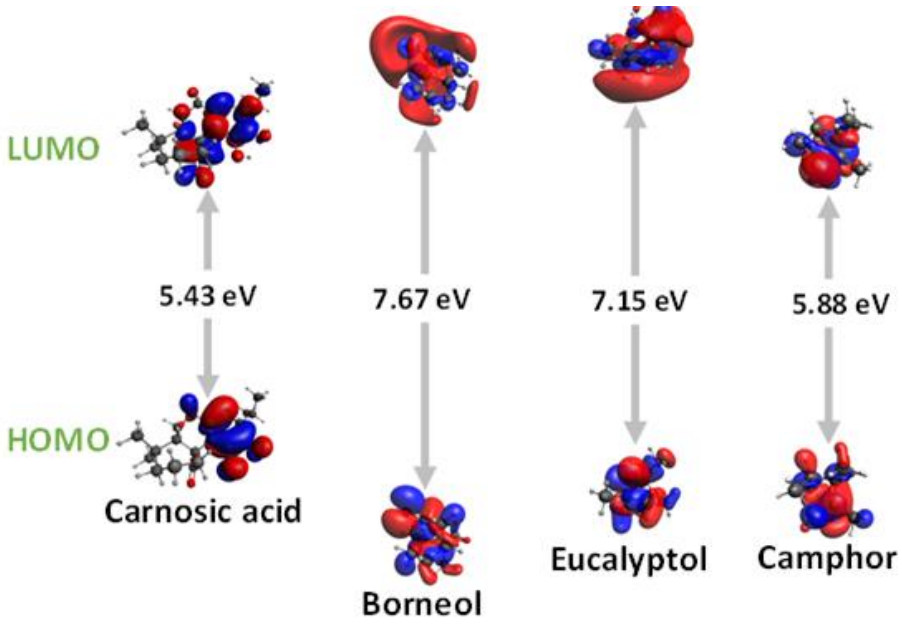

Figure 2: The calculated ground state is density surface plots for FMOs for studied drugs carnosic acid, berneol, eucalyptol, and camphor.

Recently, many reports (Novak et al. 2001; Vemuri and Makriyannis 2015) showing the correlation between FMOs and several biological mode of action such as antimicrobial, (Grover et al. 2000; Malhotra, Ravesh, and Singh 2017; Kumer, Sarker, and Paul 2019) anticancer, (Khodair et al. 2020; Kumar, Athimoolam, and Sridhar 2018; Hagar et al. 2019) antifungal (Joshi et al. 2018; Joshi et al. 2020)(41, 42)(Joshi et al. 2018; Joshi et al. 2020)(Joshi et al. 2018; Joshi et al. 2020)[41, 42][40, 41][40, 41][39, 40][39, 40][39, 40][39, 40][39, 40][39, 40][39, 40][39, 40][39, 40][38, 39][37, 38][36, 37][35, 36][34, 35][33, 34][32, 33][31, 32][30, 31][29, 30][28, 29][28, 29][28, 29][9, 10] cytotoxic (Ali et al. 2018; Rachedi et al. 2019; da Costa et al. 2018) activities and a new-drug-design field (Lewis 2003).

These reports regarding the FMOs energy levels as well as the energy gab analysis disclosed that the HOMO and the LUMO energy levels are the principle features that affect the bioactivity of small structural drug like compounds. Mostly HOMOs are the source of electrons, and, the LUMOs are electron acceptors. Clearly, the HOMO energy levels are different for all investigated compounds. The FMOs energy analysis results showed that the energies of HOMOs of drugs like carnosic acid and camphor are higher with respect to the other ingredients berneol and eucalyptol, and bernol showed the least lying HOMO. However, the carnosic acid and camphor exhibits more stabilized LUMO level compared to the rest of the compounds. The order of the energy gap is: berneol > eucalyptol > camphor > carnosic acid. Remarkably, drug like carnosic acid active ingredient of the least energy gap ΔE = 5.43 eV, with numerous hydrophilic sites for interactions that enable the binding with the receptors. This recommends that hydrophilic molecular interactions significantly influence the binding affinity of small drug like compounds to the protein receptors. HOMO of a specific

active ingredient and LUMO with neighboring residues can cause molecular orbital interactions during the protein binding process.

2.3 Chemical Reactivity Descriptors

The energy levels of the FMOs, E_{HOMO} and E_{LUMO} predict the power ionization ($I = -E_{HOMO}$) and the electronic ionization ($A = -E_{LUMO}$) of the molecules. In addition, these molecular orbitals are used to measure further descriptors of chemical reactions such as electronegativity (χ), softness (δ), global hardness (η), and electrophilicity (ω). These descriptors are estimated with the following equations: (Ortega et al. 2020).

$$\chi = -\frac{1}{2}(E_{HOMO} + E_{LUMO}) \qquad (1)$$

$$\eta = -\frac{1}{2}(E_{HOMO} - E_{LUMO}) \qquad (2)$$

$$\delta = \frac{1}{\eta} \qquad (3)$$

$$\omega = \frac{\chi^2}{2\eta} \qquad (4)$$

The χ reflects the molecule's ability to attract electrons. The global hardness (η) is a measure of the charge transfer prevention ability. The global softness (δ) indicates the ability of the molecule to acquire electrons. Due to their smaller FMOs energy gap, soft compounds are more reactive than the harder ones due to their ability to transfer electrons to the receptors. The Electrophilicity (ω) is an indicator of the reduction of the energy difference caused by to the increased transfer ability of the electron between the LUMO and HOMO.

2.4 Molecular Electrostatic Potential (MEP)

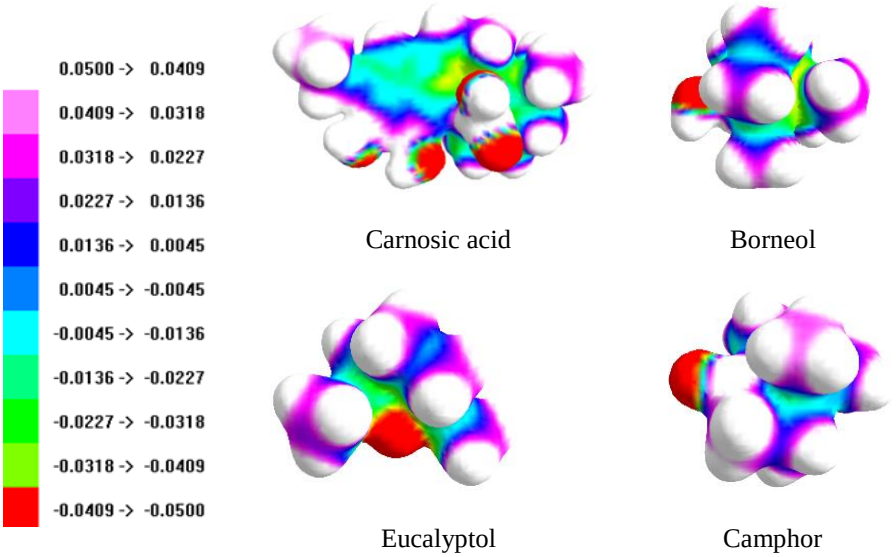

Figure 3: MEP of drugs Carnosic acid, Borneol, Eucalyptol, and Camphor.

To provide evidence for drug like active ingredient as inhibitors, MEP must be estimated. MEP provides a sign of the size, shape and nature of the electrostatic force, it is positive, negative, and neutral. These can be useful tools to predict the physicochemical properties. In addition, electrostatic precipitation can be a beneficial tool in assessing the reactivity of these compounds to attack electrophiles and nucleophiles. The molecular electrostatic potential of the studied drug like active ingredient is estimated using the identical method under the identical base sets and displayed in Figure 3. In MEP, the extreme negative zone is favored site of electrophilic attack, shown in red. Thus, the attacking electrophile is attracted

to the negatively charged locations, the blue regions. It is clear that the molecular size, shape and the direction of negative, positive and neutral electrostatic potentials vary with the compounds as a result of the type of atoms and their electronic nature. The difference in electrostatic potential mapping around the drug like compounds could be mainly responsible for the difference in the affinity for the association with the active site receptor.

2.4.1 Molecular Docking

Docking calculations were performed to obtain the SARS-CoV-2 M^{pro}-drugs binding conformation. The drugs are: carnosic acid, berneol, eucalyptol, camphor, hydroxychloroquine and favipiravir. We have used docking of the hydroxychloroquine and favipiravir into the protein sites as a control.

The binding affinity of the compounds carnosic acid, berneol, eucalyptol, and camphor were -6.9, -4.2, -4.2 and -4.4 kcal/mol, respectively, as listed in Table 3. The 2D illustrations of the binding configuration for the drugs are shown in Fig. 5 and 6. All compounds have exhibited binding with the Cys-145 catalytic dyad. Interestingly, carnosic acid binds to both catalytic dyads (Cys-145 and His-41) with hydrogen bond and π-interaction, giving rise to -6.9 kcal/mol binding energy. Thus, this ligand attained the least binding energy (−6.9 kcal/mol) and, hence, can be regarded as a potential inhibitor to SARS-CoV-2 M^{pro} compared to the hydroxychloroquine and favipiravir having binding affinities −6.1 and −5.1 kcal/mol, respectively.

Carnosic acid interacts with the receptor with Van der Waals interactions in addition to two hydrogen bonds with Leu144, and Glu166 (Figure 6). Other interactions include sigma and π interactions.

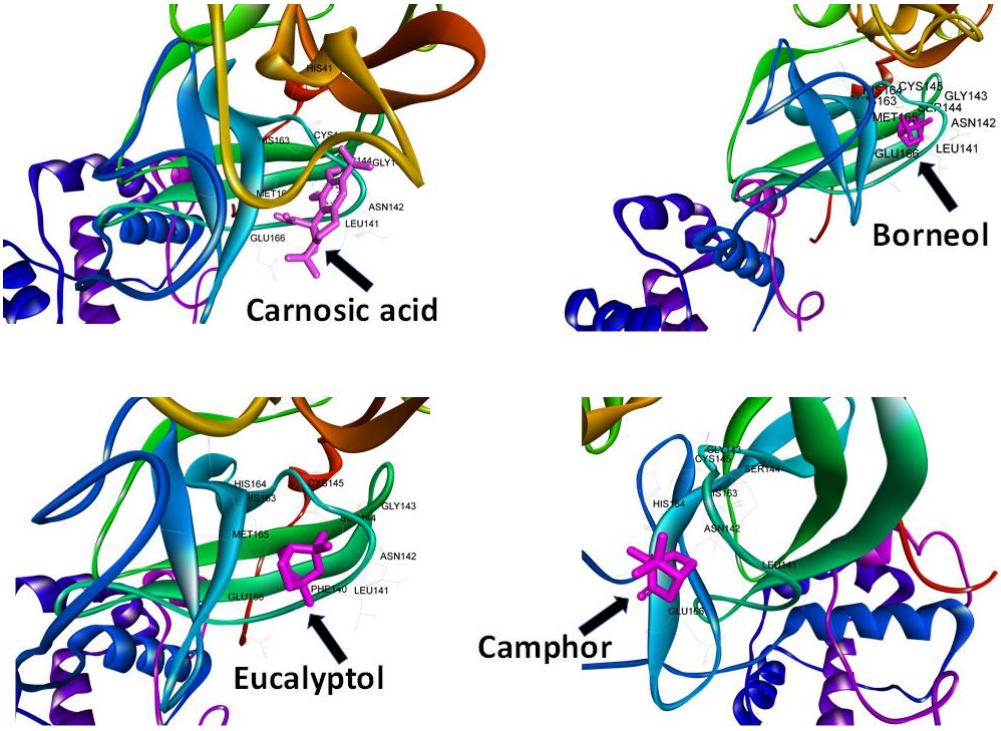

Figure 4: 3D docking models of SARS-CoV-2 M^{pro} complexes demonstrating superimposition of drugs carnosic acid (ligand 1), berneol (ligand 2), eucalyptol (ligand 3), and camphor (ligand 4) in the protein pocket. The amino acid residues (thin sticks) are indicated with the letters and numbers.

Table 3: Data analysis of the flexible docking of carnosic acid, berneol, eucalyptol, camphor, hydroxychloroquine and favipiravir in the active site of SARS-CoV-2 M^{pro} receptor.

PubChem CID	Binding affinity (kcal/mol)	Amino acid residues of SARS-CoV2 M^{pro}
65126, Carnosic acid 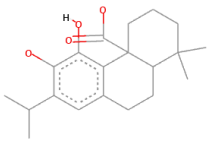	-6.9	PHE140, HIS172, HIS163, LEU141, MET165, SER144, GLU166, HIS41, LEU27, ASN142, GLY143, CYS145
64685, Borneol 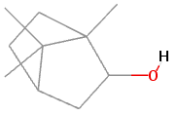	-4.2	ASN142, HIS163, LEU141, MET165, SER144, GLU166, ASN142, GLY143, CYS145
2758, Eucalyptol 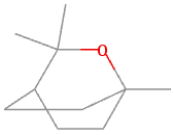	-4.2	ASN142, LEU141, CYS145, HIS163, PHE140, GLU166, HIS172, MET165, HIS164, SER144, GLY143
2537, Camphor 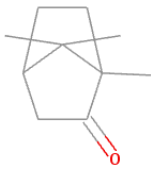	-4.4	SER144, HIS163, ASN142, HIS164, MET165, GLU166, CYS145, GLY143, LEU141, PHE140
3652, Hydroxychloroquine 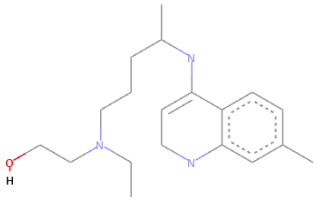	-6.1	MET49, HIS164, GLU166, HIS141, GLN189, MET165, ARG188, ASP187, HIS163, LEU141, PHE140, SER144, GLY143, CYS145, ASN142
492405, Favipiravir 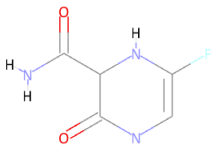	-5.1	ASN142, GLY143, SER144, HIS163, LEU141, CYS145, HIS172, GLU166, PHE140

Underlined amino acid: The most interactive amino acid in the binding pocket.

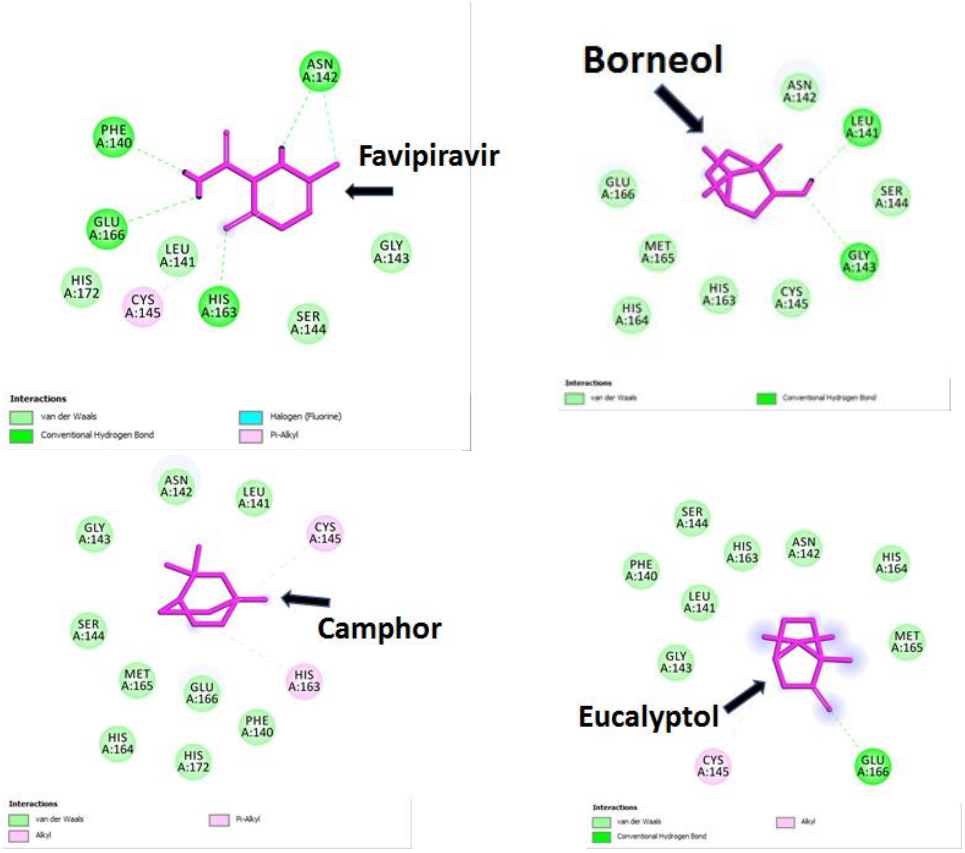

Figure 5: The interacting mode with SARS-CoV-2 M^{pro} in 2D structures in complexes with favipiravir berneol (ligand 2), eucalyptol (ligand 3), and camphor (ligand 4).

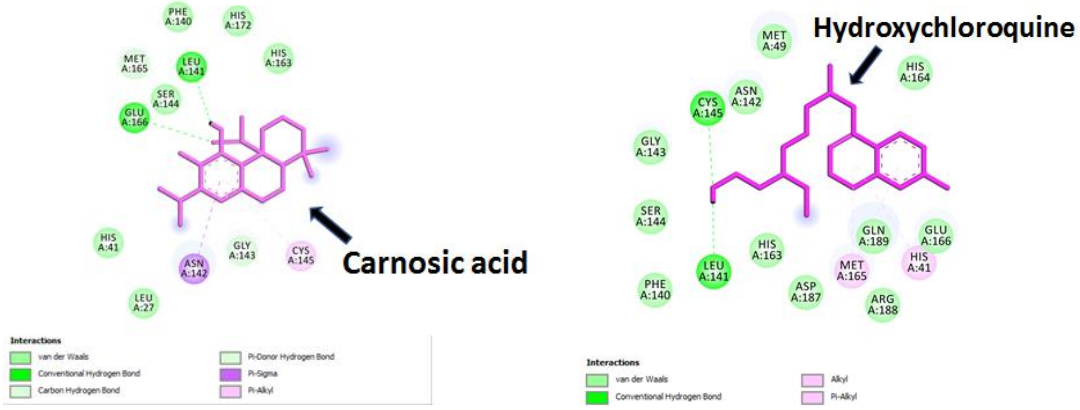

Figure 6: The interacting mode with SARS-CoV-2 M^{pro} in 2D structures of carnosic acid and hydroxychloroquine.

2.5 Materials and Methods

2.5.1 DFT Calculations

The computational ab initio calculations were performed on the drugs using ORCA software (Neese 2012). The ORCA program. (Zhu, Lopes, and MacKerell 2011). We employed the hybrid B3LYP functional and the Pople 6–311G basis set for these calculations. Initially all the structures were geometrically optimized towards the configurations with minimum energies. Visualizations of the optimized structures and frontiers orbitals (HOMO and LUMO) were done via VESTA (Heydon et al. 2001) and Avogadro packages (Hanwell et al. 2012). The calculation of the vibrational frequencies showed no negative frequencies in the results, indicating the high quality of the optimized structures. The mapping of the MEP was performed using ArgusLab software (Laxmi 2019).

2.5.2 Molecular Docking Procedure

Docking calculations were achieved using the AUTODOCK 4.2 software (Norgan et al. 2011). Using the Protein Data Bank (PDB: 6LU7): https://www.rcsb.org/structure/6LU7, the crystal structure of COVID-19 main protease at 2.16 Å resolution was obtained. The 3D structures in SDF format for all of the drugs were obtained from the PubChem database. Conversion between various file format as needed by the docking program was performed with OpenBabel software (O'Boyle et al. 2011). Before the stage of docking, the protein was prepared using Chimera program (https://www.cgl.ucsf.edu/chimera). Moreover, the water molecules were eliminated, the polarized hydrogen atoms got inserted into the amino acid residues and Gasteiger charges were added to all atoms of the protein. The ligand-protein docking was performed using a search space around the Glu-166 site. Then the resulting docked structures in PDBQT formats were used for the interaction analysis. The results analysis and visualization were performed using the Discovery Studio Visualizer v17.2.0.16349 (Studio 2008).

3. CONCLUSIONS

Rosemary is important type of the natural Lamiaceae plants with several medicinal properties, rendering it as a prospective inhibitor for the new SARS-CoV-2 virus. Nevertheless, their SARS-CoV-2 inhibition properties have not been published. In this work the inhibition efficacy for rosemary against SARS-CoV-2 has been demonstrated using systematic DFT calculations and molecular docking.

The estimated DFT data have shown that the dipole moment of the active ingredient of rosemary under investigation was in the range of 4.29-1.68 with the highest value attained by the carnosic acid. The high dipole moment for the carnosic acid may indicate its good binding affinity pose within a specific virus target receptor. Moreover, the structural complexity for the carnosic acid gave rise to its highest calculated polarizability of 225.5 $Bohr^3$ compared to the rest of the rosemary ingredients. Remarkably, the carnosic acid active ingredient contains the least energy gap between the frontier orbitals (HOMO and LUMO) of ~ 5.43 eV, with several hydrophilic sites for interactions, further enabling its binding with the virus receptors. Interestingly, and as anticipated from DFT results, molecular docking calculations showed that carnosic acid had the least binding energy (−6.9 kcal/mol) and, hence, can be regarded as a prospective inhibitor to SARS-CoV-2 main protease (M^{pro}). It binds to both M^{pro} catalytic dyads (Cys-145 and His-41) with hydrogen bond and π-interaction. This carnosic acid ligand binding quality was comparable to renowned SARS-CoV-2 drugs, hydroxychloroquine and favipiravir, having binding affinities of −6.1 and −5.1 kcal/mol, respectively.

Funding: This study was carried out without external funding.

Conflicts of Interest: The authors do not have any conflict of interest to report.

4. ACKNOWLEDGEMENT

The author is highly delighted to Dr. Mohammad Hajar, and Dr. Mohammad Khalafalla for their assistance and collaboration.

5. REFERENCES

[1] Al-Sereiti, M.; K. Abu-Amer; and P. Sena. 1999. Pharmacology of rosemary (Rosmarinus officinalis Linn.) and its therapeutic potentials.
[2] Ali, M.S.; M.A. Farah; H.A. Al-Lohedan; and K.M. Al-Anazi. 2018. Comprehensive exploration of the anticancer activities of procaine and its binding with calf thymus DNA: a multi spectroscopic and molecular modelling study. RSC advances 8:9083-9093.
[3] Amel, B. 2013. Traditional treatment of high blood pressure and diabetes in Souk Ahras District. Journal of Pharmacognosy and Phytotherapy 5:12-20.
[4] Avorn, J. 2015. The $2.6 billion pill–methodologic and policy considerations. New England Journal of Medicine 372:1877-1879.
[5] Bakırel, T.; U. Bakırel; O.Ü. Keleş; S.G. Ülgen; and H. Yardibi. 2008. In vivo assessment of antidiabetic and antioxidant activities of rosemary (Rosmarinus officinalis) in alloxan-diabetic rabbits. Journal of Ethnopharmacology 116:64-73.
[6] Borrás-Linares, I.; Z. Stojanović; R. Quirantes-Piné; D. Arráez-Román; J. Švarc-Gajić; A. Fernández-Gutiérrez; and A. Segura-Carretero. 2014. Rosmarinus Officinalis Leaves as a Natural Source of Bioactive Compounds. International Journal of Molecular Sciences 15:20585-20606.
[7] Chan, K.W.; V.T. Wong; and S.C.W. Tang. 2020. COVID-19: An update on the epidemiological, clinical, preventive and therapeutic evidence and guidelines of integrative Chinese–Western medicine for the management of 2019 novel coronavirus disease. The American journal of Chinese medicine:1-26.
[8] Cheng, F. 2019. In silico oncology drug repositioning and polypharmacology. In Cancer Bioinformatics, 243-261: Springer.

[9] Cheng, F.; H. Hong; S. Yang; and Y. Wei. 2017. Individualized network-based drug repositioning infrastructure for precision oncology in the panomics era. Briefings in bioinformatics 18:682-697.
[10] Cheng, F.; J.L. Murray; and D.H. Rubin. 2016. Drug repurposing: new treatments for zika virus infection? Trends in Molecular Medicine 22:919-921.
[11] Cheung, S. and J. Tai. 2007. Anti-proliferative and antioxidant properties of rosemary Rosmarinus officinalis. Oncology Reports 17:1525-1531.
[12] Cui, L.; M.O. Kim; J.H. Seo; I.S. Kim; N.Y. Kim; S.H. Lee; J. Park; J. Kim; and H.S. Lee. 2012. Abietane diterpenoids of Rosmarinus officinalis and their diacylglycerol acyltransferase-inhibitory activity. Food Chemistry 132:1775-1780.
[13] da Costa, R.M.; J.K. Bastos; M.C. Costa; M.M. Ferreira; C.S. Mizuno; G.F. Caramori; G.R. Nagurniak; M.R. Simão; R.A. Dos Santos; and R.C. Veneziani. 2018. In vitro cytotoxicity and structure-activity relationship approaches of ent-kaurenoic acid derivatives against human breast carcinoma cell line. Phytochemistry 156:214-223.
[14] Devaux, C.A.; J.-M. Rolain; P. Colson; and D. Raoult. 2020. New insights on the antiviral effects of chloroquine against coronavirus: what to expect for COVID-19? International Journal of Antimicrobial Agents:105938.
[15] Elhassan, I.A. and N.M. Osman. 2014. New Chemotype Rosmarinus officinalis L.(Rosemary) R. officinalis ct. bornyl acetate. American Journal of Research Communication 2:232-240.
[16] Grimstein, M.; Y. Yang; X. Zhang; J. Grillo; S.-M. Huang; I. Zineh; and Y. Wang. 2019. Physiologically based pharmacokinetic modeling in regulatory science: an update from the US Food and Drug Administration's Office of Clinical Pharmacology. Journal of Pharmaceutical Sciences 108:21-25.
[17] Grover, M.; B. Singh; M. Bakshi; and S. Singh. 2000. Quantitative structure–property relationships in pharmaceutical research–Part 1. Pharmaceutical Science & Technology Today 3:28-35.
[18] Hagar, M.; H. Ahmed; T. El-Sayed; and R. Alnoman. 2019. Mesophase behavior and DFT conformational analysis of new symmetrical diester chalcone liquid crystals. Journal of Molecular Liquids 285:96-105.
[19] Haloui, M.; L. Louedec; J.-B. Michel; and B. Lyoussi. 2000. Experimental diuretic effects of Rosmarinus officinalis and Centaurium erythraea. Journal of Ethnopharmacology 71:465-472.
[20] Hanwell, M.D.; D.E. Curtis; D.C. Lonie; T. Vandermeersch; E. Zurek; and G.R. Hutchison. 2012. Avogadro: an advanced semantic chemical editor, visualization, and analysis platform. Journal of Cheminformatics 4:17.
[21] Heydon, A.; R. Levin; T. Mann; and Y. Yu. 2001. The Vesta approach to software configuration management. Compaq. Systems Research Center [SRC].
[22] Javanmardi, J.; C. Stushnoff; E. Locke; and J.M. Vivanco. 2003. Antioxidant activity and total phenolic content of Iranian Ocimum accessions. Food Chemistry 83:547-550.
[23] Joshi, R.; A. Kumari; K. Singh; H. Mishra; and S. Pokharia. 2020. Triorganotin (IV) complexes of Schiff base derived from 1, 2, 4-triazole moiety: Synthesis, spectroscopic investigation, DFT studies, antifungal activity and molecular docking studies. Journal of Molecular Structure 1206:127639.
[24] Joshi, R.; N. Pandey; S.K. Yadav; R. Tilak; H. Mishra; and S. Pokharia. 2018. Synthesis, spectroscopic characterization, DFT studies and antifungal activity of (E)-4-amino-5-[N'-(2-nitro-benzylidene)-hydrazino]-2, 4-dihydro-[1, 2, 4] triazole-3-thione. Journal of Molecular Structure 1164:386-403.
[25] Khodair, A.I.; M.K. Awad; J.-P. Gesson; and Y.A. Elshaier. 2020. New N-ribosides and N-mannosides of rhodanine derivatives with anticancer activity on leukemia cell line: Design, synthesis, DFT and molecular modelling studies. Carbohydrate Research 487:107894.
[26] Kumar, S.S.; S. Athimoolam; and B. Sridhar. 2018. Structural, spectral, theoretical and anticancer studies on new co-crystal of the drug 5-fluorouracil. Journal of Molecular Structure 1173:951-958.
[27] Kumer, A.; M.N. Sarker; and S. Paul. 2019. The Simulating Study of HOMO, LUMO, thermo physical and Quantitative Structure of Activity Relationship (QSAR) of Some Anticancer Active Ionic Liquids. Eurasian Journal of Environmental Research 3:1-10.
[28] Laxmi, K. 2019. Structural Elucidation of Drug Aspirin by Using Various Software Tools Like HyperChem, Argus Lab, ChemSketch, Avogrado and Chemeo Database. J Theor Comput Sci 5:2.
[29] Lewis, D.F. 2003. Quantitative structure–activity relationships (QSARs) within the cytochrome P450 system: QSARs describing substrate binding, inhibition and induction of P450s. Inflammopharmacology 11:43-73.
[30] Liu, C.; Q. Zhou; Y. Li; L.V. Garner; S.P. Watkins; L.J. Carter; J. Smoot; A.C. Gregg; A.D. Daniels; and S. Jervey. 2020. Research and development on therapeutic agents and vaccines for COVID-19 and related human coronavirus diseases: ACS Publications.
[31] Liu, J.; R. Cao; M. Xu; X. Wang; H. Zhang; H. Hu; Y. Li; Z. Hu; W. Zhong; and M. Wang. 2020. Hydroxychloroquine, a less toxic derivative of chloroquine, is effective in inhibiting SARS-CoV-2 infection in vitro. Cell discovery 6:1-4.
[32] Malhotra, R.; A. Ravesh; and V. Singh. 2017. Synthesis, characterization, antimicrobial activities, and QSAR studies of organotin (IV) complexes. Phosphorus, Sulfur, and Silicon and the Related Elements 192.
[33] Neese, F. 2012. The ORCA program system. Wiley Interdisciplinary Reviews: Computational Molecular Science 2:73-78.

[34] Nishiura, H.; N.M. Linton; and A.R. Akhmetzhanov. 2020. Serial interval of novel coronavirus (COVID-19) infections. International Journal of Infectious Diseases.
[35] Norgan, A.P.; P.K. Coffman; J.-P.A. Kocher; D.J. Katzmann; and C.P. Sosa. 2011. Multilevel parallelization of AutoDock 4.2. Journal of Cheminformatics 3:12.
[36] Novak, J.; K. Zitterl-Eglseer; S.G. Deans; and C.M. Franz. 2001. Essential oils of different cultivars of Cannabis sativa L. and their antimicrobial activity. Flavour and Fragrance Journal 16:259-262.
[37] O'Boyle, N.M.; M. Banck; C.A. James; C. Morley; T. Vandermeersch; and G.R. Hutchison. 2011. Open Babel: An open chemical toolbox. Journal of Cheminformatics 3:33.
[38] Ortega, J.T.; M.L. Serrano; F.H. Pujol; and H.R. Rangel. 2020. Unrevealing sequence and structural features of novel coronavirus using in silico approaches: The main protease as molecular target. EXCLI journal 19:400.
[39] Pérez-Fons, L.; M.T. GarzÓn; and V. Micol. 2010. Relationship between the Antioxidant Capacity and Effect of Rosemary (Rosmarinus officinalis L.) Polyphenols on Membrane Phospholipid Order. Journal of Agricultural and Food Chemistry 58:161-171.
[40] Rachedi, K.O.; T.-S. Ouk; R. Bahadi; A. Bouzina; S.-E. Djouad; K. Bechlem; R. Zerrouki; T.B. Hadda; F. Almalki; and M. Berredjem. 2019. Synthesis, DFT and POM analyses of cytotoxicity activity of α-amidophosphonates derivatives: Identification of potential antiviral O, O-pharmacophore site. Journal of Molecular Structure 1197:196-203.
[41] Shetty, R.; A. Ghosh; S.G. Honavar; P. Khamar; and S. Sethu. 2020. Therapeutic opportunities to manage COVID-19/SARS-CoV-2 infection: Present and future. Indian Journal of Ophthalmology 68:693.
[42] Studio, D. 2008. Discovery Studio. Accelrys [2.1].
[43] Tu, Z.; T. Moss-Pierce; P. Ford; and T.A. Jiang. 2013. Rosemary (Rosmarinus officinalis L.) Extract Regulates Glucose and Lipid Metabolism by Activating AMPK and PPAR Pathways in HepG2 Cells. Journal of Agricultural and Food Chemistry 61:2803-2810.
[44] Vemuri, V.K. and A. Makriyannis. 2015. Medicinal chemistry of cannabinoids. Clinical Pharmacology and Therapeutics 97:553-558.
[45] Wang, M.; R. Cao; L. Zhang; X. Yang; J. Liu; M. Xu; Z. Shi; Z. Hu; W. Zhong; and G. Xiao. 2020. Remdesivir and chloroquine effectively inhibit the recently emerged novel coronavirus (2019-nCoV) in vitro. Cell Research 30:269-271.
[46] Warren, T.K.; R. Jordan; M.K. Lo; A.S. Ray; R.L. Mackman; V. Soloveva; D. Siegel; M. Perron; R. Bannister; and H.C. Hui. 2016. against Ebola virus in rhesus monkeys.
[47] Wenkert, E.; A. Fuchs; and J.D. McChesney. 1965. Chemical Artifacts from the Family Labiatae. The Journal of Organic Chemistry 30:2931-2934.
[48] Yang, P. and X. Wang. 2020. COVID-19: a new challenge for human beings. Cellular & Molecular Immunology:1-3.
[49] Yao, X.; F. Ye; M. Zhang; C. Cui; B. Huang; P. Niu; X. Liu; L. Zhao; E. Dong; and C. Song. 2020. In vitro antiviral activity and projection of optimized dosing design of hydroxychloroquine for the treatment of severe acute respiratory syndrome coronavirus 2 (SARS-CoV-2). Clinical Infectious Diseases.
[50] Yesil-Celiktas, O.; C. Sevimli; E. Bedir; and F. Vardar-Sukan. 2010. Inhibitory Effects of Rosemary Extracts, Carnosic Acid and Rosmarinic Acid on the Growth of Various Human Cancer Cell Lines. Plant Foods for Human Nutrition 65:158-163.
[51] Zhang, L. and Y. Liu. 2020. Potential interventions for novel coronavirus in China: a systemic review. Journal of Medical Virology.
[52] Zhou, D.; P. Zhang; C. Bao; Y. Zhang; and N. Zhu. 2020. Emerging understanding of etiology and epidemiology of the novel coronavirus (COVID-19) infection in Wuhan, China.
[53] Zhou, Y.; Y. Hou; J. Shen; Y. Huang; W. Martin; and F. Cheng. 2020. Network-based drug repurposing for novel coronavirus 2019-nCoV/SARS-CoV-2. Cell discovery 6:1-18.
[54] Zhu, N.; D. Zhang; W. Wang; X. Li; B. Yang; J. Song; X. Zhao; B. Huang; W. Shi; and R. Lu. China Novel Coronavirus I, Research T (2020) A novel coronavirus from patients with pneumonia in China, 2019. New England Journal of Medicine 382:727-733.
[55] Zhu, X.; P. Lopes; and A. MacKerell. 2011. Wiley Interdisciplinary Reviews: Computational Molecular Science.